ELSEVIER

International Journal of Heat and Fluid Flow 21 (2000) 456–462

International Journal of HEAT AND FLUID FLOW

www.elsevier.com/locate/ijhff

A procedure for the routine calculation of laminar free and mixed convection in inclined ducts

B.J. Brinkworth *

University of Wales, P.O. Box 685, Cardiff CF2 3TA, UK

Received 15 May 1999; accepted 4 March 2000

Abstract

A procedure is described for rapidly estimating the flow-rate and heat transfer for laminar free and mixed convection in inclined ducts. Solutions are given by closed-form expressions, suitable for routine use at spreadsheet level. The flow-rate is obtained by equating the sum of the pressure differences which drive the flow with that of those opposing it. Among the former, the contribution of free convection is represented by superposing a pressure difference equal to that due to buoyancy in a static column of fluid of the same height as the duct. In the initial development it is assumed that wall friction and heat transfer may be represented by expressions for forced convection, including entrance effects. The procedure is tested against CFD results for a vertical parallel-plate duct with heat flux at one wall only. Despite the severity of the case, agreement is found to be sufficiently good to validate the method for routine initial design and optimisation studies for most conditions of free and mixed convection. Discrepancies become noticeable only at high Grashof number, where the buoyancy component is high enough to produce substantial asymmetry in the velocity profile.

1. Introduction

A new technical situation has required an old problem to be revisited. In building-integrated photovoltaic installations, cooling ducts are generally fitted behind the panels, to assist in regulating the temperature rise due to the absorption of that part of the solar radiation which is not converted into electricity (Brinkworth et al., 1997). Routine methods are needed for designing these ducts, in particular for choosing optimum dimensions for the duct.

The flow of air through such a duct is primarily due to buoyancy induced by heat transfer from the panels, but may be enhanced by a pressure difference caused by local wind effects. The general situation is depicted in Fig. 1. The principal design case, when the maximum temperature rise is experienced, is in still-air conditions, when the flow is exclusively buoyancy-induced. However, the effect of the varying temperature on the efficiency of energy conversion in the panels requires that for prediction of long-term performance the flow and heat transfer in the duct must be evaluated for all states. These include those in which buoyancy and wind effects are combined, and sometimes of comparable magnitude. Thus design methods are needed which allow these mixed-flow conditions to be calculated routinely.

Flow and heat transfer for situations of free and mixed convection in ducts (the latter meaning forced convection accompanied by buoyancy effects) have been extensively researched since at least the 1940s (Elenbaas, 1942), and several valuable summaries of this work have been compiled (Rohsenow and Hartnett, 1973; Shah and London, 1978; Kakac et al., 1987). Possible combinations of duct shape and orientation, and of wall and entry boundary conditions are very numerous. Conditions over part or all of the duct length are those of simultaneous development of the velocity and temperature fields in the fluid, requiring representation in two or three dimensions. Except for the limiting cases of fully developed flow, therefore, the solutions have been obtained mainly by numerical CFD methods.

Obtaining results from the literature applicable to a particular problem can be frustrating. Very few have been tabulated in any detail, so that for the most part results are presented only in graphical form, and appear on a minuscule scale, limiting the reliability with which information may be extracted. Solutions in an explicit, preferably analytic, form would be very valuable for routine use, even if some degree of approximation had to be accepted. A method which serves this purpose by the superposition of the principal effects is described here. The driving forces are expressed by the difference in wind pressures at the inlet and outlet locations, and by an equivalent pressure difference to represent the driving due to buoyancy. Resistance to flow is expressed in terms of the pressure-losses due to inlet effects and wall friction. The main conjectures concerning the process have been supported by experiment (Brinkworth et al., 1999). Further discussion of the method follows, with representations illustrating the effects of the various influences, and comparisons with CFD simulations.

* Tel.: +44-1222-874-797; fax: +44-1222-874-317.
E-mail address: brinkworthbj@cardiff.ac.uk (B.J. Brinkworth).

0142-727X/00/$ - see front matter
PII: S0142-727X(00)00027-8

Notation

A	dimensionless group for free convection, Eq. (18)
B	dimensionless group for forced convection, Eq. (19)
b	depth of parallel-plate duct
c_p	specific heat capacity of fluid
D	hydraulic diameter of duct cross-section
f	wall friction coefficient, Eq. (3)
f_{app}	apparent value of f for duct including entrance effects, Eq. (11)
f_d	suffix denoting condition in fully developed flow
Gr_D	Grashof number for free convection, Eq. (9)
g	acceleration due to gravity
k	thermal conductivity of fluid
k_h	coefficient for Δp_h, Eq. (6)
k_i	coefficient for Δp_i, Eq. (14)
L	length of duct
L^+	dimensionless duct length, Eq. (4)
L^*	modified dimensionless duct length, L^+/Pr
Nu	local Nusselt number for wall heat transfer, Eq. (21)
Nu_{fd}	local Nusselt number for fully developed laminar flow
Pr	Prandtl number of fluid
q	wall heat flux
Re_D	Reynolds number of flow, Eq. (5)
S	stratification parameter for temperature in fluid column, Eq. (2)
T_b	wall temperature at adiabatic surface of duct
T_e	bulk mean temperature of fluid at exit from duct
T_i	mean temperature of fluid at entry to duct
T_m	local bulk mean temperature of fluid
T_{mean}	bulk mean temperature of column of fluid
T_0	wall temperature at heated surface of duct
u	mean velocity of fluid
u_0	uniform velocity of fluid at entry to duct
x	local axial distance from entry to duct
Y	dimensionless position across duct from heated surface, Eq. (23)
y	position across duct from heated surface
β	coefficient of volumetric expansion of fluid (taken $1/T$ for air)
Δp_b	pressure difference due to buoyancy
Δp_e	externally applied pressure difference for forced convection
Δp_f	pressure drop due to wall friction
Δp_h	pressure drop due to hydraulic losses
Δp_i	pressure drop in fluid approaching duct inlet
ν	kinematic viscosity of fluid
ρ	density of fluid
θ	inclination of duct axis to horizontal
Θ	dimensionless wall temperature, Eq. (20)
Θ_b	value of Θ at adiabatic wall
Θ_0	value of Θ at heated wall

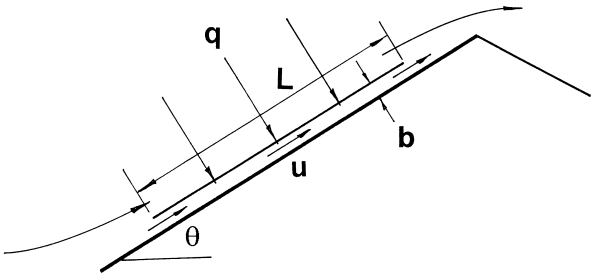

Fig. 1. General arrangement of PV cooling duct.

2. Superposition

The relative contributions of free and forced convection effects in driving the flow are often represented by the ratio of the Grashof and Reynolds numbers, usually in the form of Gr/Re or Gr/Re^2 (Bejan, 1995), though other scales have been shown to be relevant also (Yao, 1983). Accordingly, there has been a tendency to give results in terms of this ratio (e.g., Aung and Worku, 1987). This is, however, not a convenient form for the user, since the value of the flow-rate is an outcome of the process and hence the Re is not known a priori. In superposition, the driving forces for free and forced convection are represented separately, in terms of known quantities. This approach has been used occasionally from early times, particularly for routine design of ventilation systems (ASHRAE, 1985) and in the analysis of flow in thermosiphon loops, such as may arise in turbine blades, reactors and solar thermal systems (see reviews by Japiske, 1973; Norton and Probert, 1986). It allows an essentially one-dimensional treatment to be used, yielding a closed-form analytical expression for the flow-rate. However, the boundaries within which these solutions may be regarded as sufficiently accurate for regular use do not seem to have been established. This is addressed below for the cases studied.

The pressure drop available to drive the flow is the sum of that due to external pressures and an equivalent term representing the buoyancy forces. This is equated to the sum of the pressure drops due to friction and other hydraulic losses

$$\Delta p_e + \Delta p_b = \Delta p_f + \Delta p_h. \tag{1}$$

It is conjectured that the buoyancy contribution is effectively equal to the pressure difference between the base and the top of a static column of fluid of the duct height, so that

$$\begin{aligned}\Delta p_b &= \rho g \beta (T_{mean} - T_i) L \sin\theta \\ &= \rho g \beta S (T_e - T_i) L \sin\theta,\end{aligned} \tag{2}$$

where $S(T_e - T_i)$ is the mean temperature rise of the fluid in the column. The value of S depends on the profile of temperature rise through the height of the column (Brinkworth et al., 1999); for example, for a linear temperature rise, $S = 0.5$.

The pressure drop along a duct due to wall friction can be expressed (in the Darcy formulation) by

$$\Delta p_f = f(L/D)(\rho u^2/2). \tag{3}$$

Values for the friction coefficient f collected for various duct shapes generally take the form of the product fRe_D as a function of the dimensionless duct length

$$f\,Re_D = fn(L^+) = fn(L/D\,Re_D) \tag{4}$$

and

$$Re_D = uD/\nu \tag{5}$$

with D the hydraulic diameter of the duct (4 × cross-sectional area/perimeter).

The pressure drop Δp_h arises from other hydraulic losses, which are generally represented by coefficients k_h referenced to the dynamic head of the flow, so that

$$\Delta p_h = \sum k_h \rho u^2/2. \tag{6}$$

We now consider some solutions of Eq. (1) for a representative case, which are then compared with others that have been

reported or with newly generated numerical results, to establish the boundaries of acceptable approximation by the superposition method.

3. Flow-rate estimation

3.1. The parallel-plate duct

Among the standard cases dealt with in the literature, (e.g., Aung, 1972) the nearest to the practical situation which gives rise to the study is that of a uniform duct formed between wide parallel-plates, with a uniform heat flux (UHF) at one wall and the other adiabatic. It is chosen also as providing the most severe test of the method, since it results in the greatest temperature asymmetry across the duct for a given heat input. If the depth of the duct transverse to the flow is b, then $D = 2b$ for this case. The streamwise temperature variation is linear in this case so that $S = 0.5$, and for a heat flux q the mean temperature rise is

$$T_e - T_i = 2qL/\rho Duc_p. \tag{7}$$

3.2. Superposition in fully developed free-convective flow

For this case, Δp_e is zero, $f\,Re_D = 96$ and Δp_h is negligible, so Eq. (1) gives

$$2g\beta qL\sin\theta/\rho c_p = (96/Re_D)u^3,$$

which, after some manipulation, can be seen to take the dimensionless form

$$(L^+)^2 = 48\ Pr/Gr_D\sin\theta, \tag{8}$$

where the Grashof number for the UHF wall condition is

$$Gr_D = g\beta qD^5/Lv^2k. \tag{9}$$

Hence the development yields a relationship of the conventional kind, $Gr = fn$ (geometry, Re, Pr).

For a vertical duct, Eq. (8) becomes

$$(L^+)^2 = 48\ Pr/Gr_D. \tag{10}$$

Expressions obtained by Aung (1972) for this case reduce to the form of Eq. (10) when the same definitions for Gr_D and L^+ are used, and thus the approach is supported. It is noted however that for the UHF condition, the gradient of mean temperature, and hence the pressure gradient due to buoyancy, is constant along the duct, as is the case also for the friction term in fully developed flow. Thus a conjecture that the terms for the two components may be equated might reasonably be asserted for this condition. It is next to be seen whether this is also a fair approximation for the conditions of developing flow in finite ducts. The sin θ dependence on inclination, shown in Eq. (8), is already well attested by measurement on natural convection flows at least down to $\theta \sim 30°$ (Azevedo and Sparrow, 1985; Brinkworth et al., 1999), so the comparisons which follow are made for vertical ducts only.

3.3. Superposition in developing flow

In forced convection, a fully developed condition is reached only in long ducts, typically of dimensionless length L^+ not less than about 0.05 in the limit of an isothermal flow. In the entrance region at the beginning of the duct, the rate of pressure drop is greater than in fully developed flow. This is due partly to the velocity gradient at the wall (and hence the shear stress) being higher than in the fully developed region, and partly to the increase in momentum flux as the velocity profile develops. The flow in the entrance region is affected by the geometry of the entrance aperture, and when there is heat transfer by the simultaneous development of the velocity and temperature boundary layers. The number of possible conditions is considerable, but not many cases of these simultaneously developing laminar flows have been calculated (Shah and London, 1978; Kakac et al., 1987).

For present purposes, it is convenient to have the pressure drop along the duct represented by the apparent value f_{app} of the friction factor over the length L of the duct (Kays, 1966), defined in the Darcy formulation by

$$\Delta p_f = f_{app}(L/D)\rho u^2/2. \tag{11}$$

For parallel-plate ducts, it is clear from the above that the product $f_{app}Re_D$ must merge with the value 96 when L^+ is large and the flow is fully developed over most of its length. Order-of-magnitude calculations show that for cases of practical interest involving PV cooling ducts, L^+ will not normally be lower than about 0.01. No tabulated values have been found for simultaneously developing flow, but for isothermal flow with L^+ above about 0.01, Kakac et al. (1987) report that a good representation is that

$$f_{app}Re_D = 96 + 0.674/L^+, \tag{12}$$

where the constant 0.674 is identified with the pressure defect number $K(\infty)$. If this were to remain a fair approximation for the case with heat transfer, then equating Δp_f to Δp_b for a vertical duct, we obtain, for comparison with Eq. (10), that

$$(L^+)^2 = (48 + K(\infty)/2L^+)Pr/Gr_D. \tag{13}$$

For inclined ducts, Gr_D becomes $Gr_D\sin\theta$, as before. From Eq. (13), the value of L^+ can be determined for given driving conditions (Gr_D), and from L^+ the value of Re_D and hence the mean velocity and the flow-rate are obtained for the given duct geometry (L/D).

The case of vertical ducts has been calculated by Aung et al. (1972). However, their results are given only in graphical form and cannot be scanned accurately enough to provide a real test of Eq. (13). Accordingly, a new set of data has been calculated, using a similar numerical CFD procedure (simultaneous solution of the equations of continuity, momentum and energy, subject to the prescribed boundary conditions and the requirements of uniform mass flow-rate and linearly increasing enthalpy flux). These are compared with results from Eq. (13) in Fig. 2(a). In this, and all subsequent figures, the full line represents the prediction and the points the results obtained by CFD. The results given are obtained partly to compare with those of Aung et al. (1972), for the case with a starting condition of a uniform velocity u_0 across the duct and local ambient pressures at inlet and outlet. As far as can be ascertained by scaling from published illustrations, the numerical results are identical with these.

However, especially for short ducts, the choice of inlet and outlet conditions can significantly affect the results (Tichy, 1983; Naylor et al., 1991). It is then necessary to include the hydraulic losses term, as in Eq. (1). For the comparison of Fig. 2(b), account is taken of the pressure drop Δp_i necessary for the fluid to reach the inlet velocity, which might be expressed as

$$\Delta p_i = k_i\rho u_0^2/2 \tag{14}$$

leading to

$$(L^+)^2 = (48 + (K(\infty) + k_i)/2L^+)Pr/Gr_D. \tag{15}$$

For a fluid undergoing a slow (isothermal) expansion from the surroundings, $k_i = 1$, giving, with the appropriate value for $K(\infty)$,

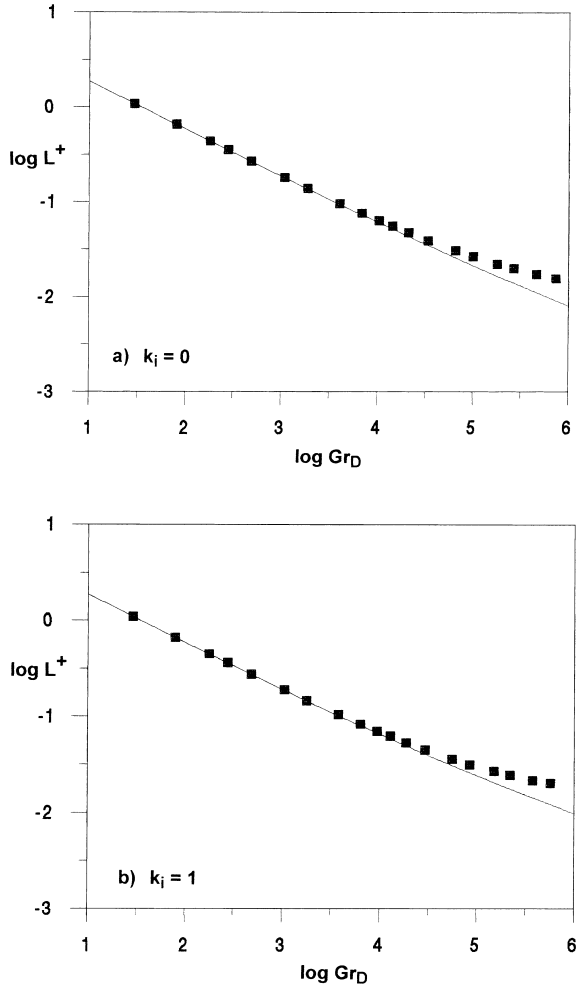

Fig. 2. Free convection flow prediction for vertical duct (a) $k_i = 0$ and (b) $k_i = 1$

$$(L^+)^2 = (48 + 0.837/L^+)Pr/Gr_D. \tag{16}$$

This relation is compared with the computed values for the same entry condition in Fig. 2(b).

Fig. 2(a) and (b) shows that the approach by superposition gives very good estimates for free convective flow in finite ducts. At high Gr_D the L^+ is somewhat underestimated, and hence the flow-rate obtained is overestimated. A glance at the velocity profiles shows the reason (e.g., see Fig. 3). The asymmetry induced by high heat flux results in a higher velocity gradient at the heated wall and a lower one at the insulated wall. The latter does not quite compensate for the former, so that the overall wall friction is greater than that obtained for isothermal flow, Eq. (12). It is remarked that because of the strong asymmetry induced by having heat input at one wall only, the case chosen here to illustrate the superposition approach is a particularly taxing one.

Fig. 2 indicates that the effect of the velocity distortion on the prediction of the flow does not become noticeable until Gr_D is greater than about 10^5. In this region, the L^+ values are low, and for values below 0.01, unless the duct is short relative to its width, it is likely that the limit of Re_D for laminar flow will be reached. Thus, it may be concluded that agreement is good throughout the practical range of laminar free convection.

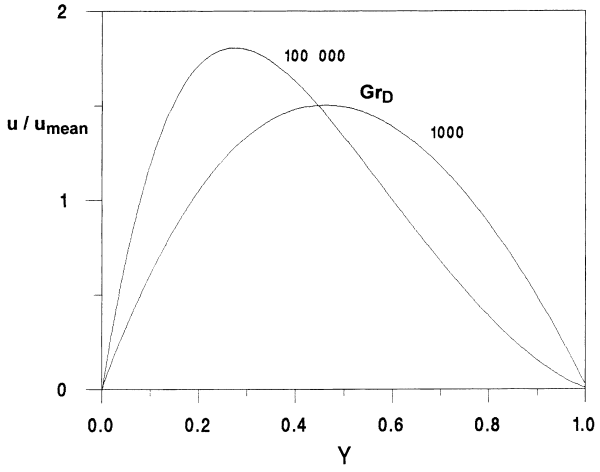

Fig. 3. Velocity profiles in free convective flow.

3.4. Superposition in mixed flow

When the driving force is augmented by an externally applied pressure difference Δp_e, the complete form of Eq. (1) is required. Manipulated into a form convenient for solution, this gives

$$A(L^+)^3 + B(L^+)^2 - 48L^+ - 0.837 = 0, \tag{17}$$

where

$$A = Gr_D/Pr \tag{18}$$

and

$$B = \Delta p_e D^4/\rho\nu^2 L^2. \tag{19}$$

The group identified here as B does not seem to have arisen previously as a parameter in this field (though the same form emerges as the dimensionless pressure difference in the computational procedure).

Eq. (17) may be solved readily (for example, by the Newton–Raphson method) to obtain L^+ for the situation concerned, and hence the value of Re_D and the flow-rate, as before. For inclined ducts, the Grashof number is modified by the sin θ term, as noted above. Fig. 4 gives an illustration of how the results for vertical ducts obtained with Eq. (17) compare with values from CFD computations for a range of

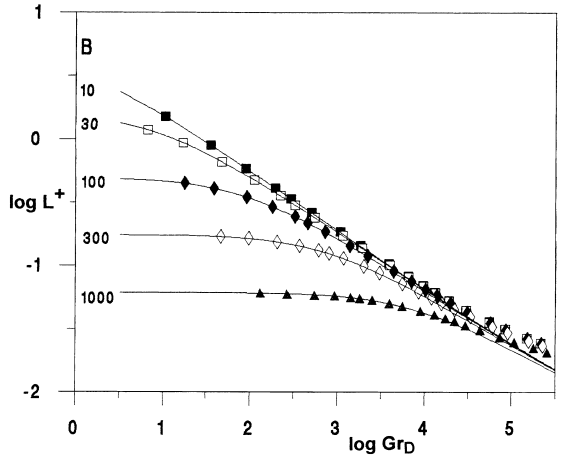

Fig. 4. Mixed convection flow prediction for vertical duct.

values of the external pressure difference parameter B. It is seen that excellent agreement is obtained throughout the mixed-flow field.

The value of Δp_i used in the illustration is that for an unhindered expansion by the air approaching the duct. The superposition procedure conveniently allows for other hydraulic loss terms to be included in Δp_h, if desired. For example, based on measurements, engineering texts suggest a typical additional loss for a sharp-edged entrance of $0.5\rho u_0^2/2$, which perhaps originates in recirculation zones which have been noted to occur just inside the entrance (Straatman et al., 1994), though this would not be shown with the CFD scheme used and cannot be tested here. Pressure changes may occur at the exit also, depending on its geometry, and could also be incorporated by inserting an appropriate k_h value if desired. For this study, it has been assumed that the pressure in the plane of the outlet equals the local ambient pressure, with no additional loss or pressure recovery.

4. Heat transfer

4.1. The required quantities

The usual requirement in practice is to be able to determine the wall temperatures on the two sides of the duct, T_0 and T_b. These may be represented in the dimensionless form

$$\Theta = (T - T_i)/(qb/k) = 2(T - T_i)/(qD/k). \tag{20}$$

Alternatively, for the heated surface, the local Nusselt number may be defined in terms of the difference between the wall temperature and the local bulk mean fluid temperatute T_m

$$Nu = (qD/k)/(T_0 - T_m)_x = 2/(\Theta_0 - \Theta_m)_x. \tag{21}$$

4.2. Fully developed flow

The temperature distribution across the duct can be obtained analytically for fully developed flow, for example by solving the energy equation in conjunction with a parabolic (Hagen–Poiseuille) velocity distribution (Bejan, 1995). For the parallel-plate duct heated from one side, this gives the profile

$$(T_0 - T)_{fd} = (qD/k)\{(Y/2) - (Y^3/2) + (Y^4/4)\}, \tag{22}$$

where

$$Y = y/b \tag{23}$$

so that

$$(T_0 - T_m)_{fd} = (qD/k)(13/70) \tag{24}$$

leading to

$$Nu_{fd} = 70/13 = 5.385 \tag{25}$$

and

$$(T_b - T_m)_{fd} = -(qD/k)(9/140). \tag{26}$$

For the UHF condition, T_m increases linearly with duct length, which in conjunction with Eqs. (24) and (26) provides the dimensionless forms

$$\Theta_0 = (4/Pr)L^+ + (13/35) \tag{27}$$

and

$$\Theta_b = (4/Pr)L^+ - (9/70). \tag{28}$$

Using Eq. (25), these may be rendered alternatively as

$$\Theta_0 = (4/Pr)L^+ + (2/Nu_{fd}) \tag{29}$$

and

$$\Theta_b = (4/Pr)L^+ - (9/13Nu_{fd}). \tag{30}$$

4.3. Free convection

One of the assumptions made in modelling the flow is that the dependence of the wall friction on L^+ could be taken to remain effectively the same however the flow is generated – by free, forced or mixed convection. The corresponding assumption for the heat transfer would be that the dependence of Nu on L^+ would be similarly invariant. Data for the parallel-plate duct with UHF on one side are very sparse (Heaton et al., 1964; Kakac et al., 1987; Shah and London, 1978), but for L^+ greater than 0.01, a fair approximation to those available is

$$Nu = 5.385 + 0.015/L^+. \tag{31}$$

(The scaling laws require that the dependency is more correctly in terms of $L^* = L^+/Pr$ (Bejan, 1995), but since all the work here is for air flows, the data are more conveniently rendered in the form of Eq. (31), the numerator of the second term being evaluated by taking $Pr = 0.7$.) It is now supposed that the duct wall temperatures will be given approximately by expressions similar to Eqs. (29) and (30), but using the local Nu as in Eq. (31), with L^+ related to Gr_D via Eq. (16), as before. This proposition is tested for the case of vertical ducts in Fig. 5, which shows the maximum values of dimensionless temperature obtained for the two walls, as found at the exit of the duct. These are shown together with CFD results, as for the flow predictions. Insofar as the numerical values can be compared with lines scaled from published illustrations, these are identical with those of Aung et al. (1972).

The agreement with CFD simulation is again found to be good, at least up to Gr_D of about 10^4, where the distortion of the velocity profile begins to take effect. (The representation for Θ_b has to be discontinued around $Gr_D \sim 10^5$, since by the procedure it is thereafter rendered negative, but this region is not of much practical interest, as the low values of Θ_b indicated show that the temperature of the cooler wall has barely risen from the value at inlet).

4.4. Mixed convection

As seen in the flow modelling, the good agreement obtained for free convection suggests that the procedure should be applicable also for mixed flows, since for a given buoyancy

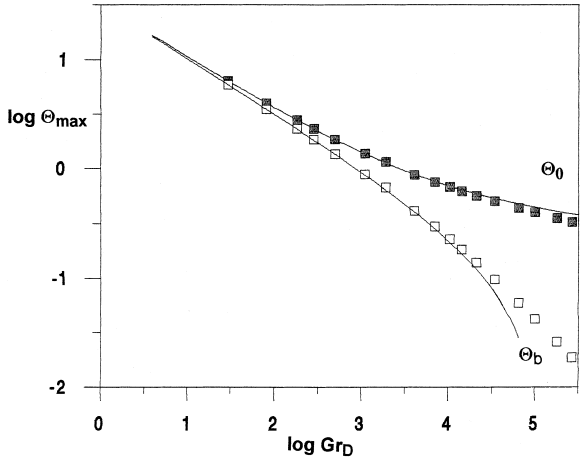

Fig. 5. Maximum wall temperature prediction – free convection in vertical duct.

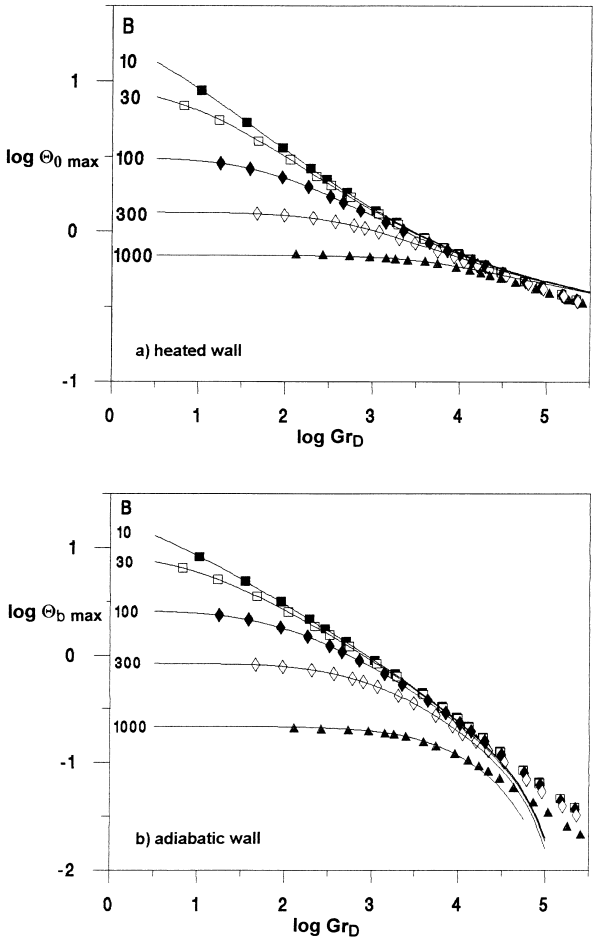

Fig. 6. Maximum wall temperature prediction – mixed convection in vertical duct: (a) heated wall and (b) adiabatic wall.

component the addition of an external pressure difference should result in less overall distortion of the velocity distribution. The determination of the appropriate value of L^+ to be inserted in Eq. (31) is now via Eq. (17). Comparison of the predicted dimensionless temperatures with the results obtained by CFD are shown for the hotter wall in Fig. 6(a) and for the cooler wall in Fig. 6(b). The agreement is seen to be very good over most of the field, the departure being again confined to the region involving high Grashof number.

5. Comment

The procedure described results, in its most general form, in a cubic equation for the flow, Eq. (17) here, which is readily solved. By comparison with numerical computations, it is indicated that the method is able to give a representation of the flow and heat transfer that is quite good enough for preliminary design work, and especially for optimisation studies, in which a large number of cases need to be scanned quickly. The expressions required are straightforward and give the solutions in closed form, so that the procedure can be used routinely at the spreadsheet level. Further, conditions in practice are never quite as severe as in the case used for validation here. Some of the heat input is necessarily transferred to the rear wall by radiation, reducing the variation of temperature across the duct for a given overall heat flux (Liu and Sparrow, 1980). The variation of the body force due to buoyancy is correspondingly less and hence the velocity profile is less distorted in practice than in these comparisons. Thus the range of Grashof number over which the approximation is good will be somewhat greater than is indicated here.

The method described uses expressions for wall friction and heat transfer for a corresponding isothermal case. It is not to be expected that these would remain entirely unaltered by the gross distortion of the velocity profile that occurs with strong buoyancy, particularly in the case of heat transfer from one side only, though the temperature profiles in mixed convective flows are known to vary less than the distortion of the velocity profiles might suggest (Hewitt et al., 1996). The direction of the deviation from CFD results shows that both friction and heat transfer are increased by the presence of buoyancy, as is well attested by other work, both for the entrance and the fully developed region (Rao and Morris, 1967; Cebeci and Bradshaw, 1984; Yan, 1995). Nevertheless, a version of the procedure has been well validated by experiment over a wide range of operating conditions for inclined ducts with a trapezoidal cross-section (Brinkworth et al., 1999). The measurements indicate that flow and heat transfer are adequately represented by the expressions appropriate for that duct section in isothermal flow, and confirm some of the other assumptions, for example that the buoyancy term for an inclined duct depends on the duct height $L \sin \theta$ (down to 30° to the horizontal, the lowest value used).

6. Conclusion

It is concluded that a practical closed-form procedure has been described for the routine calculation of the flow and heat transfer in developing free and mixed laminar convection in ducts. Expressions for the flow are obtained by equating the pressure differences driving the flow with those corresponding to the induction at the entrance and the frictional resistance of the duct. The basic assumptions are: (a) that a pressure difference equal to that due to buoyancy in a static column of fluid can be superposed upon any external pressure difference to represent the free convection driving component and (b) that the friction factor and Nusselt number relations applicable are those already known for isothermal forced convection.

The procedure is tested against numerical CFD results, for the case of a parallel-plate duct heated from one side only. Despite the severity of the case, very satisfactory agreement is found, both for the flow-rate and wall temperature predictions. Deviations begin to occur only for high values of Grashof number (beyond $\sim 10^5$ for flow, $\sim 10^4$ for temperatures), where the distortion of the velocity profile due to the asymmetric heating becomes substantial. Though practical situations which prompted the study rarely fall into this region, there are indications that the method is able to provide useful predictions there also.

References

ASHRAE Handbook, 1985. Fundamentals. ASHRAE, Atlanta, GA.

Aung, W., 1972. Fully developed laminar free convection between vertical plates heated asymmetrically. Int. J. Heat Mass Trans. 15, 1577–1580.

Aung, W., Fletcher, L.S., Sernas, V., 1972. Developing laminar free convection between vertical flat plates with asymmetric heating. Int. J. Heat Mass Trans. 15, 2293–2308.

Aung, W., Worku, G., 1987. Mixed convection in ducts with asymmetric wall heat fluxes. ASME J. Heat Trans. 109, 947–951.

Azevedo, L.F.A., Sparrow, E.M., 1985. Natural convection in open-ended inclined channels. ASME J. Heat Trans. 107, 893–901.

Bejan, A., 1995. Convection Heat Transfer, second ed. Wiley, New York.

Brinkworth, B.J., Cross, B.M., Marshall, R.H., Yang, H., 1997. Thermal regulation of photovoltaic cladding. Solar Energy 61, 169–178.

Brinkworth, B.J., Marshall, R.H., Ibarahim, Z., 1999. A validated model of naturally ventilated PV cladding. Solar Energy (in press).

Cebeci, T., Bradshaw, P., 1984. Physical and Computational Aspects of Convective Heat Transfer. Springer, New York.

Elenbaas, W., 1942. Heat dissipation of parallel-plates by free convection. Physica 9, 1–23.

Heaton, H.S., Reynolds, W.C., Kays, W.M., 1964. Heat transfer in annular passages simultaneous development of velocity and temperature filelds in laminar flow. Int. J. Heat Mass Trans. 7, 763–781.

Hewitt, G.F., Shires, G.L., Polezhaev, Y.V. (Ed.), 1996. International Encyclopedia of Heat and Mass Transfer. CRC Press, Boca Raton.

Japiske, G., 1973. Advances in thermosyphon technology. In: Invine, T.F., Hartnett, J.P. (Eds.), Advances in Heat Transfer, vol. 9. Academic Press, New York, pp. 1–111.

Kakac, S., Shah, R.K., Aung, W. (Ed.), 1987. Handbook of Single-phase Convective Heat Transfer. Wiley, New York.

Kays, W.M., 1966. Convective Heat and Mass Transfer. McGraw-Hill, New York.

Liu, C.H., Sparrow, E.M., 1980. Convective – radiative interaction in a parallel-plate channel – application to air-operated solar collectors. Int. J. Heat Mass Trans. 23, 1137–1146.

Naylor, D., Floryan, J.M., Tarasuk, J.D., 1991. A numerical study of developing free convection between isothermal vertical plates. ASME J. Heat Trans. 113, 620–626.

Norton, B., Probert, S.D. 1986. Thermosyphon solar energy water heaters. In: Boer, K.W. (Ed.), Advances in Solar Energy, vol. 3. Plenum Press, New York, pp. 125–170.

Rao, T.L.S., Morris, W.D., 1967. Superimposed laminar forced and free convection between vertical parallel-plates when one plate is uniformly heated and the other is thermally insulated. Proc. Inst. Mech. Engr. 182 (3H), 374–381.

Rohsenow, W.M., Hartnett, J.P. (Ed.), 1973. Handbook of Heat Transfer. McGraw-Hill, New York.

Shah, R.K., London, A.L., 1978. Laminar flow forced convection in ducts. Supplement 1 to Advances in Heat Transfer. Academic Press, New York.

Straatman, A.G., Naylor, D., Floryan, J.M., Tarasuk, J.D., 1994. A study of natural convection between inclined isothermal plates. ASME J. Heat Trans. 116, 243–245.

Tichy, J.A., 1983. The effect of inlet and exit losses on free convective laminar flow in the Trombe wall channel. ASME J. Solar Energy Eng. 105, 187–193.

Yan, W.-M., 1995. Transport phenomena of developing laminar mixed convection heat and mass transfer in inclined rectangular ducts. Int. J. Heat Mass Trans. 38, 2905–2914.

Yao, L.S., 1983. Free and forced convection in the entry region of a heated vertical channel. Int. J. Heat Mass Trans. 26, 65–72.